IEEE Access
Multidisciplinary | Rapid Review | Open Access Journal

Received April 21, 2018, accepted May 23, 2018, date of publication May 29, 2018, date of current version July 6, 2018.

Digital Object Identifier 10.1109/ACCESS.2018.2841994

Sliding Mode Control Based on Dynamic Model for Transport Vehicle

CHUNBO XIU[1,2], AND RUOSI WANG[1]

[1]School of Electrical Engineering and Automation, Tianjin Polytechnic University, Tianjin 300387, China
[2]Key Laboratory of Advanced Electrical Engineering and Energy Technology, Tianjin Polytechnic University, Tianjin 300387, China

Corresponding author: Chunbo Xiu (xiuchunbo@tjpu.edu.cn)

This work was supported in part by the Natural Science Foundation of Tianjin under Grant 17JCYBJC18500 and in part by the Program for Innovative Research Team in University of Tianjin under Grant TD13-5036.

ABSTRACT In order to improve the control performance of the transport vehicle, the dynamic model, instead of the kinematic model, is established. The equation of state can be divided into two independent subsystems: the speed sub system and the attitude angle sub system. The sliding mode controls based on the dynamic model are designed for the two subsystems to reduce the complexity of the overall system, and the armature voltages of the motors are used as the control inputs of the system of the transport vehicle. The disturbances, for instance the fluctuations in the power supply, are considered, so the control law has robustness to the external disturbances. Simulation results show that the control method can control the transport vehicle to move according to the desired signals, and the validity of the method can be proved.

INDEX TERMS Dynamic model, sliding mode control, transport vehicle.

I. INTRODUCTION

At present, the application of robots has been rapidly expanded from the early fixed robotic arm in the industrial production line to the complex autonomous mobile robots. Mobile robots have been widely used in many fields [1]– [3], such as rescue, life service and commercial application. As a typical nonlinear nonholonomic system with the time varying and strong coupling [4], [5], the mobile robot involves many complex control problems. Therefore, it has been one of the research hot spots to control the mobile robot effectively [6], [7]. The transport vehicle which is an under-actuated system is also a classical type of mobile robot. There are some uncertain disturbances which would cause bad effects on control performance in the system. Though PID control can meet the control requirements in the common condition [8], [9], many advanced control methods [10]–[13] are explored and used to control the transport vehicle to improve the control performance of the system. Among them, sliding mode control is one of effective methods, which has strong robustness to the external disturbance and the parametric variation [14]–[17]. Sliding mode control has extensive application in the field of scientific research, such as in power system, new fuel, communication and image processing [18]–[21], and it is more often used to resolve the control problem of the under-actuated system [22]–[24]. Therefore, the sliding mode control is chosen to control the attitude angle and speed of the transport vehicle in this paper.

Generally, the attitude control of the transport vehicle can be designed based on either the dynamics model or the kinematics model [24], [25]. However, the controller designed based on the kinematics model can be only used when the transport vehicle works under constraint the condition of the lower speed, the lower acceleration and the lower load [26], [27]. Otherwise, the control performance would degrade obviously [28].

For this, a novel sliding mode control strategy is proposed to control the transport vehicle. The speed sub system and the attitude angle sub system are decoupled to simplify the system. Some disturbances, for instance the uncertain fluctuations in the power supply, are considered, and the sliding mode control based on the dynamic model is used to improve the robustness the system. The attitude angle and speed of the transport vehicle is controlled by directly using the voltages of the drive motors as control inputs. The control strategy has the good robustness and feasibility.

II. THE SIMPLIFIED MODEL OF THE TRANSPORT VEHICLE

The simplified geometry model of the transport vehicle is shown in Figure 1. The vehicle is composed of two driving wheels, one front universal wheel and the car body. The two driving wheels are respectively driven by two DC motors.

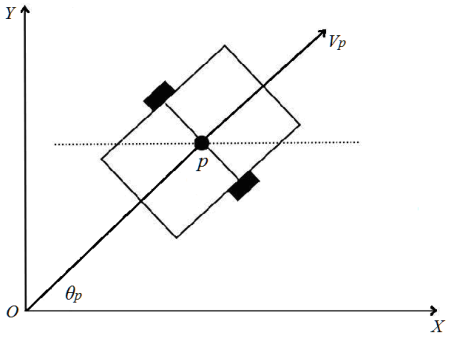

FIGURE 1. The simplified geometric model of the transport vehicle

The swerve of the car body is controlled by the differential control of the two driving wheels. The radius of the car wheel is r, the wheelbase of the two wheels is l, the mass of the wheel is m, and the mass of the car body is M_P.

In Fig. 1, the coordinate system XOY is established. The center of mass of the transport vehicle is set as the point p, the attitude angle between the car body and the horizontal axis is set as θ_p, and the velocity of the transport vehicle is set as V_p. When the motion control of the transport vehicle is studied, the transport vehicle can be simplified as the mass point p, and the state of the transport vehicle can be described as the vector $[\mathrm{X\ Y}\ \theta_p]^{\mathrm{T}}$.

The significance of establishing the dynamic model of the transport vehicle is that the relationship between the motor voltage and the speed and angle of the vehicle can be directly established. Compared with the common control methods based on the kinematic model, the control method based on the dynamic model can reduce some uncertain intermediate links, and the control performance can be improved.

A. FORCE ANALYSIS OF THE WHEEL

Force analysis of the wheel is shown in Fig. 2. The coordinate system with the origin at the center of the wheel is set up. The left wheel is taken as an example to study the force analysis. The forces on the left wheel contain the gravity $m_L g$, the support force from the ground F_{fL}, the pressure from the car body F_{pL}, and the driving torque τ_L of the left wheel.

The Newton-Euler equation of the left wheel can be established as follows:

$$F_{fL}^z = F_{pL}^z + m_L g \tag{1}$$
$$F_{fL}^x - F_{pL}^x = m_L a_L \tag{2}$$
$$F_{fL}^y = F_{pL}^y \tag{3}$$
$$\tau_L - F_{fL}^x r = J_{yL}\dot{\omega}_L \tag{4}$$

where, J_{yL} indicates the rotational inertia of the left wheel around the Y axis. F_{fL}^x, F_{fL}^y and F_{fL}^z are separately component forces of F_{fL} along the X-axis, the Y-axis and the Z-axis. F_{pL}^x, F_{pL}^y and F_{pL}^z are separately component forces of F_{pL} along the X-axis, the Y-axis and the Z-axis. a_L indicates the acceleration of the left wheel.

Force analysis of the right wheel is the same as the left wheel as:

$$F_{fR}^z = F_{pR}^z + m_R g \tag{5}$$
$$F_{fR}^x - F_{pR}^x = m_R a_R \tag{6}$$
$$F_{fR}^y = F_{pR}^y \tag{7}$$
$$\tau_R - F_{fR}^x r = J_{yR}\dot{\omega}_R \tag{8}$$

where, the forces on the right wheel contain the gravity m_Rg, the support force from the ground F_{fR}, the pressure from the car body F_{pR}, and the driving torque τ_R of the right wheel. F_{fR}^x, F_{fR}^y and F_{fR}^z are separately component forces of F_{fR} along the X-axis, the Y-axis and the Z-axis. F_{pR}^x, F_{pR}^y and F_{pR}^z are separately component forces of F_{pR} along the X-axis, the Y-axis and the Z-axis. a_R indicates the acceleration of the right wheel.

B. FORCE ANALYSIS OF THE VEHICLE BODY

Force analysis of the car body is shown in Fig. 3. The coordinate system with the origin at the center of mass is set up. The directions of the coordinate systems of the car body and the wheel are same. The forces on the car body contain the gravity $M_p g$ and the two support forces from the wheels F_L and F_R.

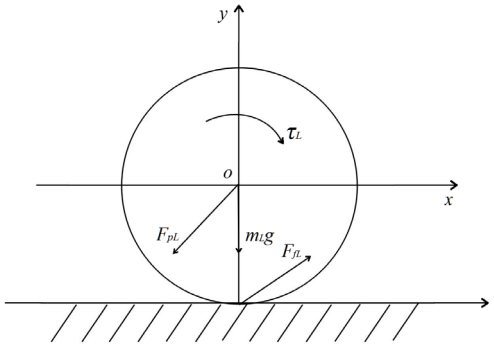

FIGURE 2. Force analysis of the wheel.

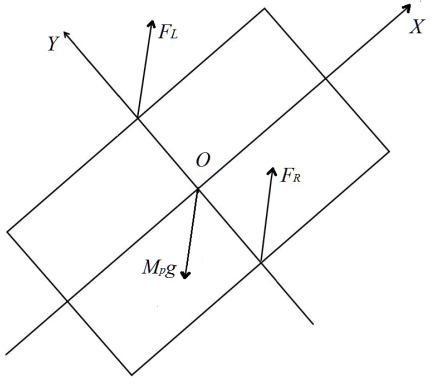

FIGURE 3. Force analysis of the car body.

The Newton-Euler equation of the car body is established as follows:

$$F_L^x + F_R^x = M_p \dot{V}_p \tag{9}$$
$$F_L^y + F_R^y = 0 \tag{10}$$
$$F_L^z + F_R^z = M_p g \tag{11}$$
$$F_R^x \frac{l}{2} - F_L^x \frac{l}{2} = J_{zL} \ddot{\theta}_p \tag{12}$$

where, J_{zL} indicates the rotational inertia of the left wheel around the Z axis. F_L^x, F_L^y and F_L^z indicate the forces of the vehicle body from the left wheel along the X-axis, Y-axis and the Z-axis, respectively. F_R^x, F_R^y and F_R^z indicate the forces of the vehicle body from the right wheel along the X-axis, the Y-axis and Z-axis, respectively.

The forces between the vehicle body and the wheel are action and reaction, that is,

$$\begin{cases} F_L = F_{pL} \\ F_R = F_{pR} \end{cases} \tag{13}$$

The speed and the attitude angle of the vehicle body can be described as:

$$V_p = \frac{r}{2}(\omega_L + \omega_R) \tag{14}$$
$$\dot{\theta}_p = \frac{r}{l}(\omega_L - \omega_R) \tag{15}$$

where, l is the wheelbase of the two wheels. The friction between the wheel and the ground is a sliding friction, so the accelerations of the two wheels center can be described as:

$$a_L = r\dot{\omega}_L \tag{16}$$
$$a_R = r\dot{\omega}_R \tag{17}$$

where, a_L and a_R represent the acceleration of the center of mass of the left wheel and right wheel, respectively.

C. DYNAMICS ANALYSIS OF THE MOTOR

The wheels of the transport vehicle are driven by two DC motors. The dynamic characteristics of the left motor can be described as:

$$\tau_L = k_{TL} i_L \tag{18}$$
$$u_L = L_{aL} \frac{di_L}{dt} + R_{aL} i_L + k_{eL} \omega_L \tag{19}$$

where, τ_L is the driving torque of the left motor, i_L is the armature current of the left motor, k_{TL} is the torque constant of the left motor, L_{aL} is the inductance of the left armature circuit, R_{aL} is the resistance of the left armature circuit, k_{eL} is the back electromotive force constant of the left motor, ω_L is the angular velocity of the left motor which is equal to the velocity of the left wheel, and u_L is the input voltage of the left motor.

According to Eq. (18) and Eq. (19), the dynamic model of the left motor with the voltage as input can be described as:

$$u_L = L_{aL} \frac{1}{k_{TL}} \frac{d\tau_L}{dt} + R_{aL} \frac{\tau_L}{k_{TL}} + k_{eL} \omega_L \tag{20}$$

Similarly, the dynamic model of the right motor can be described as:

$$u_R = L_{aR} \frac{1}{k_{TR}} \frac{d\tau_R}{dt} + R_{aR} \frac{\tau_R}{k_{TR}} + k_{eR} \omega_R \tag{21}$$

III. THE ATTITUDE CONTROL OF THE TRANSPORT VEHICLE

In this paper, sliding mode control method, which applies to the under-actuated system and is robustness to both the external disturbance and the parametric variation, is used to control the attitude of the transport vehicle. The control process is composed of the approaching the sliding surface and the converging to the equilibrium point along the sliding surface.

According to the Eq. (20) and Eq. (21), the dynamic equations of the motors can be derived as:

$$\mathbf{u} = \begin{bmatrix} u_L \\ u_R \end{bmatrix} = \frac{L_a}{k_T} A \begin{bmatrix} \ddot{\omega}_L \\ \ddot{\omega}_R \end{bmatrix} + \frac{R_a}{k_T} A \begin{bmatrix} \dot{\omega}_L \\ \dot{\omega}_R \end{bmatrix} + k_e \begin{bmatrix} \omega_L \\ \omega_R \end{bmatrix} \tag{22}$$

where,

$$A = \begin{bmatrix} J_y + mr^2 + \frac{r^2}{l^2} J_z + \frac{r^2}{4} M_p & \frac{r^2}{4} M_p - \frac{r^2}{l^2} J_z \\ \frac{r^2}{4} M_p - \frac{r^2}{l^2} J_z & J_y + mr^2 + \frac{r^2}{l^2} J_z + \frac{r^2}{4} M_p \end{bmatrix} = \begin{bmatrix} a_1 & a_2 \\ a_2 & a_1 \end{bmatrix}$$

The transport vehicle is bilateral symmetry, that is, $J_{yL} = J_{yR}$, $J_{zL} = J_{zR}$, so,

$$A = \begin{bmatrix} J_y + mr^2 + \frac{r^2}{l^2} J_z + \frac{r^2}{4} M_p & \frac{r^2}{4} M_p - \frac{r^2}{l^2} J_z \\ \frac{r^2}{4} M_p - \frac{r^2}{l^2} J_z & J_y + mr^2 + \frac{r^2}{l^2} J_z + \frac{r^2}{4} M_p \end{bmatrix} = \begin{bmatrix} a_1 & a_2 \\ a_2 & a_1 \end{bmatrix}$$

Set $x_1 = \omega_L$, $x_2 = \dot{x}_1 = \dot{\omega}_L$, $x_3 = \omega_R$, $x_4 = \dot{x}_3 = \dot{\omega}_R$ $u = \begin{bmatrix} u_L & u_R \end{bmatrix}^T$. The state equation of the transport vehicle can be described as:

$$\dot{X} = \begin{bmatrix} 0 & 1 & 0 & 0 \\ -\frac{k_e k_T}{L_a} b_1 & -\frac{R_a}{L_a} & -\frac{k_e k_T}{L_a} b_2 & 0 \\ 0 & 0 & 0 & 1 \\ -\frac{k_e k_T}{L_a} b_2 & 0 & -\frac{k_e k_T}{L_a} b_1 & -\frac{R_a}{L_a} \end{bmatrix} X + \begin{bmatrix} 0 & 0 \\ \frac{k_T}{L_a} b_1 & \frac{k_T}{L_a} b_2 \\ 0 & 0 \\ \frac{k_T}{L_a} b_2 & \frac{k_T}{L_a} b_1 \end{bmatrix} u \tag{23}$$

where, $u = \begin{bmatrix} u_L & u_R \end{bmatrix}^T$, u_L and u_R represent the voltages of the left and right wheel motors, respectively. Set $A^{-1} = B = \begin{bmatrix} b_1 & b_2 \\ b_2 & b_1 \end{bmatrix}$.

Considering some uncertain disturbances for instance fluctuations in the power supply and combining Eq. (14) and

Eq. (15), the state equation of the transport vehicle can be reestablished as:

$$\dot{X} = \begin{bmatrix} 0 & 1 & 0 & 0 & 0 \\ -\frac{k_e k_T}{L_a}(b_1+b_2) & -\frac{R_a}{L_a} & 0 & 0 & 0 \\ 0 & 0 & 0 & 1 & 0 \\ 0 & 0 & 0 & 0 & 1 \\ 0 & 0 & 0 & -\frac{k_e k_T}{L_a}(b_1-b_2) & -\frac{R_a}{L_a} \end{bmatrix} X + \begin{bmatrix} 0 & 0 \\ \frac{rk_T}{2L_a}(b_1+b_2) & \frac{rk_T}{2L_a}(b_1+b_2) \\ 0 & 0 \\ 0 & 0 \\ \frac{rk_T}{lL_a}(b_1-b_2) & -\frac{rk_T}{lL_a}(b_1-b_2) \end{bmatrix} \begin{bmatrix} u_L+d_1 \\ u_R+d_2 \end{bmatrix} \quad (24)$$

where, $x_1 = v, x_2 = \dot{v}, x_3 = \theta, x_4 = \dot{\theta}, x_5 = \ddot{\theta}$, d_1 and d_2 are respectively the fluctuations of voltages u_L and u_R. $|d_1| < D_1$, $|d_2| < D_2$, and D_1, D_2 are the boundaries of disturbances.

Generally, the armature voltages of DC motors are usually controlled by pulse width modulation (PWM) method. When the power supply fluctuates, the same the duty cycle maybe corresponds to different output voltage. Therefore, the disturbances d_1 and d_2 correspond with the actual situation.

Because there is no coupling between the speed and the attitude angle in Eq. (23), the equation of state can be divided into two independent subsystems: the speed sub system and the attitude angle subsystem which can be respectively controlled by the sliding mode control to reduce the complexity of the overall system.

A. SLIDING MODE CONTROL OF THE SPEED SUB SYSTEM

The state equation of the speed sub system can be described as:

$$\begin{bmatrix} \dot{v} \\ \ddot{v} \end{bmatrix} = \begin{bmatrix} 0 & 1 \\ -\frac{k_e k_T}{L_a}(b_1+b_2) & -\frac{R_a}{L_a} \end{bmatrix} \begin{bmatrix} v \\ \dot{v} \end{bmatrix} + \begin{bmatrix} 0 & 0 \\ \frac{rk_T}{2L_a}(b_1+b_2) & \frac{rk_T}{2L_a}(b_1+b_2) \end{bmatrix} \begin{bmatrix} u_L+d_1 \\ u_R+d_2 \end{bmatrix} \quad (25)$$

For simplicity, the sliding surface is chosen as:

$$s_1(x) = ce_v(x) + \dot{e}_v(x) \quad (26)$$

In Eq. (25), the parameter c should meet the Hurwitz condition which can ensure s_1 to be a stable sliding surface.

Set Lyapunov function as:

$$V = \frac{1}{2}s_1^2 \quad (27)$$

Then,

$$\begin{aligned} \dot{s}_1(x) &= c\dot{e}_v(x) + \ddot{e}_v(x) \\ &= -\frac{k_e k_T}{L_a}(b_1+b_2)v + \left(c - \frac{R_a}{L_a}\right)\dot{v} \\ &\quad + \frac{rk_T}{2L_a}(b_1+b_2)u_1 + \frac{rk_T}{2L_a}(b_1+b_2)(d_1+d_2) \\ &\quad - c\dot{v}_d - \ddot{v}_d \end{aligned} \quad (28)$$

where, $u_1 = u_L + u_R$. And the control law can be designed as:

$$\begin{aligned} u_1 &= \frac{2k_e}{r}v + \frac{2(R_a - cL_a)}{rk_T(b_1+b_2)}\dot{v} + \frac{2cL_a}{rk_T(b_1+b_2)}\dot{v}_d \\ &\quad + \frac{2L_a}{rk_T(b_1+b_2)}\ddot{v}_d - (D_1+D_2)\,\mathrm{sgn}(s_1) \end{aligned} \quad (29)$$

Thus,

$$s_1\dot{s}_1 = -s_1 \cdot \frac{rk_T(b_1+b_2)}{2L_a}((d_1+d_2) - (D_1+D_2)\,\mathrm{sgn}(s_1)) < 0$$

Therefore, $\dot{V} \leq 0$ and the equality holds up if and only if s_1=0. The reachability of the sliding surface can be proved.

B. SLIDING MODE CONTROL OF THE ATTITUDE ANGLE SUB SYSTEM

The state equation of the attitude angle subsystem can be described as:

$$\begin{bmatrix} \dot{\theta} \\ \ddot{\theta} \\ \dddot{\theta} \end{bmatrix} = \begin{bmatrix} 0 & 1 & 0 \\ 0 & 0 & 1 \\ 0 & -\frac{k_e k_T}{L_a}(b_1-b_2) & -\frac{R_a}{L_a} \end{bmatrix} \begin{bmatrix} \theta \\ \dot{\theta} \\ \ddot{\theta} \end{bmatrix} + \begin{bmatrix} 0 & 0 \\ 0 & 0 \\ \frac{rk_T}{lL_a}(b_1-b_2) & -\frac{rk_T}{lL_a}(b_1-b_2) \end{bmatrix} \begin{bmatrix} u_L+d_1 \\ u_R+d_2 \end{bmatrix} \quad (30)$$

Similarly, the sliding surface is chosen as:

$$s_2(x) = c_1 e_\theta(x) + c_2 \dot{e}_\theta(x) + \ddot{e}_\theta(x) \quad (31)$$

In Eq. (30), the parameters c_1 and c_2 should also meet the Hurwitz condition which can ensure s_2 to be a stable sliding surface.

Set Lyapunov function as:

$$V = \frac{1}{2}s_2^2 \quad (32)$$

Then,

$$\begin{aligned} \dot{s}_2(x) &= c_1\dot{e}_\theta(x) + c_1\ddot{e}_\theta(x) + \dddot{e}_\theta(x) \\ &= \frac{c_1 L_a - k_e k_T(b_1-b_2)}{L_a}\dot{\theta} + \frac{c_2 L_a - R_a}{L_a}\ddot{\theta} \\ &\quad + \frac{rk_T}{lL_a}(b_1-b_2)u_2 + \frac{rk_T(b_1-b_2)}{lL_a}(d_1-d_2) \\ &\quad - c_1\dot{\theta}_d - c_2\ddot{\theta}_d - \dddot{\theta}_d \end{aligned} \quad (33)$$

where, $u_2 = u_L$-u_R. And the control law is designed as:

$$\begin{aligned} u_2 &= -\frac{c_1 lL_a - k_e k_T l(b_1-b_2)}{rk_T(b_1-b_2)}\dot{\theta} + \frac{c_2 lL_a - lR_a}{rk_T(b_1-b_2)}\ddot{\theta} \\ &\quad + \frac{c_1 lL_a}{rk_T(b_1-b_2)}\dot{\theta}_d + \frac{c_2 lL_a}{rk_T(b_1-b_2)}\ddot{\theta}_d + \frac{lL_a}{rk_T(b_1-b_2)}\dddot{\theta}_d \\ &\quad - (D_1+D_2)\,\mathrm{sgn}(s_2) \end{aligned} \quad (34)$$

Then,

$$s_2\dot{s}_2 = -s_2 \cdot \frac{rk_T}{lL_a}(b_1-b_2)((d_1+d_2) - (D_1+D_2)\,\mathrm{sgn}(s_2)) < 0$$

Therefore $\dot{V} \leq 0$, and the equality holds up if and only if s_2=0. Likewise, the reachability of the sliding surface can be proved.

The control voltages u_1 and u_2 can be determined by the voltages of the right and the left motors u_L and u_R as follows:

$$\begin{cases} u_1 = u_L + u_R \\ u_2 = u_L - u_R \end{cases} \tag{35}$$

Thus, the voltages of the right and the left motors u_L and u_R can be obtained as:

$$\begin{cases} u_L = \dfrac{u_1 + u_2}{2} \\ u_R = \dfrac{u_1 - u_2}{2} \end{cases} \tag{36}$$

According to Eq. (28), Eq. (33) and Eq. (35), the control laws of the left and right motors can be designed as:

$$\begin{aligned} u_L = \frac{1}{2}\Bigg[& \frac{2k_e}{r}v + \frac{2\left(R_a - cL_a\right)}{rk_T\left(b_1 + b_2\right)}\dot{v} + \frac{2cL_a}{rk_T\left(b_1 + b_2\right)}\dot{v}_d \\ & + \frac{2L_a}{rk_T\left(b_1 + b_2\right)}\ddot{v}_d - \left(D_1 + D_2\right)\operatorname{sgn}\left(s_1\right) \\ & - \frac{c_1 lL_a - k_e k_T l\left(b_1 - b_2\right)}{rk_T\left(b_1 - b_2\right)}\dot{\theta} + \frac{c_2 lL_a - lR_a}{rk_T\left(b_1 - b_2\right)}\ddot{\theta} \\ & + \frac{c_1 lL_{\mathrm{a}}}{rk_T\left(b_1 - b_2\right)}\dot{\theta}_d + \frac{c_2 lL_a}{rk_T\left(b_1 - b_2\right)}\ddot{\theta}_d \\ & + \frac{lL_a}{rk_T\left(b_1 - b_2\right)}\dddot{\theta}_d - \left(D_1 + D_2\right)\operatorname{sgn}(s_2)\Bigg] \end{aligned} \tag{37}$$

$$\begin{aligned} u_R = \frac{1}{2}\Bigg[& \frac{2k_e}{r}v + \frac{2\left(R_a - cL_a\right)}{rk_T\left(b_1 + b_2\right)}\dot{v} + \frac{2cL_a}{rk_T\left(b_1 + b_2\right)}\dot{v}_d \\ & + \frac{2L_a}{rk_T\left(b_1 + b_2\right)}\ddot{v}_d - \left(D_1 + D_2\right)\operatorname{sgn}\left(s_1\right) \\ & + \frac{c_1 lL_a - k_e k_T l\left(b_1 - b_2\right)}{rk_T\left(b_1 - b_2\right)}\dot{\theta} - \frac{c_2 lL_a - lR_a}{rk_T\left(b_1 - b_2\right)}\ddot{\theta} \\ & - \frac{c_1 lL_a}{rk_T\left(b_1 - b_2\right)}\dot{\theta}_d - \frac{c_2 lL_a}{rk_T\left(b_1 - b_2\right)}\ddot{\theta}_d \\ & - \frac{lL_a}{rk_T\left(b_1 - b_2\right)}\dddot{\theta}_d + \left(D_1 + D_2\right)\operatorname{sgn}(s_2)\Bigg] \end{aligned} \tag{38}$$

Thus, the speed and attitude angle of the transport vehicle can be directly controlled by the armature voltages of the left and the right motors. In the actual physical implementation process, the control inputs can be obtained by adjusting the PWM duty cycles of the left and the right motors. Because the disturbance caused by the fluctuation of the power supply is considered, the control method above would have the good robustness.

IV. EXPERIMENTAL SIMULATION

The correctness of the dynamic model and the feasibility of the control method are verified by the simulation experiment. The actual parameters of the transport vehicle are set as: l=0.6m, r=0.08m, m=1.5kg, M_p=60kg, c=2, c_1=2.1, c_2=2.3. The desired speed is v_d=0.1sin(t), and the desired attitude angle is θ_d=0.1sin(t). External disturbances are set as d_1=0.2sin(t) and d_2=0.5cos(t).

The control results of the speed and the attitude angle are shown in Fig.4 and Fig. 5.

From Fig. 4 and Fig. 5, though there are uncertain disturbances in the transport vehicle, both the speed and the attitude angle of the transport vehicle can track the desired signals by the sliding mode control designed in this paper.

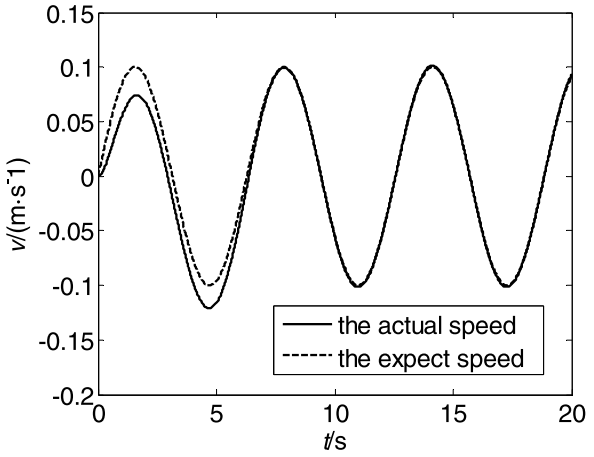

FIGURE 4. The control result of the speed.

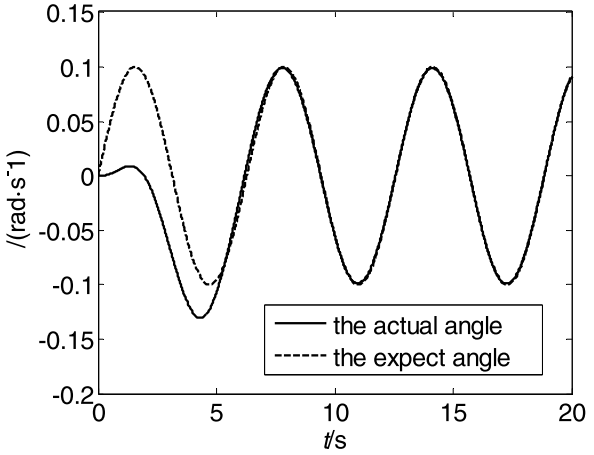

FIGURE 5. The control result of the attitude angle.

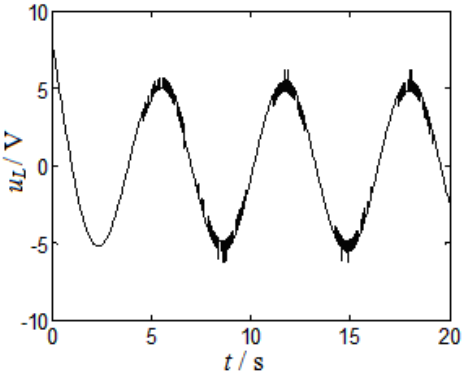

FIGURE 6. The control voltage of the left motor.

The control voltages of the left and the right motors are shown in Fig. 6 and Fig. 7.

From Fig. 6 and Fig. 7, the amplitudes the control voltages are smaller, and the proposed method is easy to

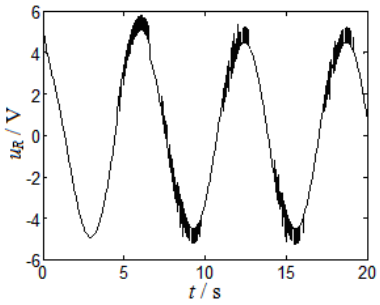

FIGURE 7. The control voltage of the right motor.

be implemented. Therefore, the validity of the sliding mode control method based on the dynamic model can be verified by the simulations.

V. CONCLUSION

A sliding mode control method based on the dynamic model, instead of the kinematic model, is proposed to improve the control performance of the transport vehicle. The armature voltages of the motors are chosen as the control inputs, and the control laws are separately designed for the speed and the attitude angle of the transport vehicle. Simulation experiments are used to prove the validity of the control method. The experimental results show that the desired speed and angle can be quickly reached and the attitude angle control of the transport vehicle can be implemented, and the control method has good robustness to the disturbances caused by the fluctuations of the power supply. So the control method can be used in the automated guided vehicle. Furthermore, the design of the sliding mode control with the optimal energy is the subsequent research direction and deserves our further exploration.

REFERENCES

[1] F. Adelhedi, A. Jribi, Y. Bouteraa, and N. Derbel, "Adaptive sliding mode control design of a SCARA robot manipulator system under parametric variations," *J. Eng. Sci. Technol. Rev.*, vol. 8, no. 5, pp. 117–123, Feb. 2015.

[2] M. Chen, "Robust tracking control for self-balancing mobile robots using disturbance observer," *IEEE/CAA J. Automatica Sinica*, vol. 4, no. 3, pp. 458–465, Feb. 2017.

[3] A. R. da Silva and A. M. C. Machado, "Control of mobile robots with Amorphic Architecture," *IEEE Latin Amer. Trans.*, vol. 14, no. 7, pp. 3093–3101, Jul. 2016.

[4] X. Yu and L. Liu, "Target enclosing and trajectory tracking for a mobile robot with input disturbances," *IEEE Control Syst. Lett.*, vol. 1, no. 2, pp. 221–226, Oct. 2017.

[5] H. Wang, D. Guo, X. Liang, W. Chen, G. Hu, and K. K. Leang, "Adaptive vision-based leader-follower formation control of mobile robots," *IEEE Trans. Ind. Electron.*, vol. 64, no. 4, pp. 2893–2902, Apr. 2017.

[6] Z. Peng, S. Yang, G. Wen, A. Rahmani, and Y. Yu, "Adaptive distributed formation control for multiple nonholonomic wheeled mobile robots," *Neurocomputing*, vol. 173, pp. 1485–1494, Jan. 2016.

[7] X. P. Meng *et al.*, "Motion control of robot based on a new integral separated PID," *Int. J. Wireless Mobile Comput.*, vol. 11, no. 3, pp. 207–213, Feb. 2016.

[8] M. Mendoza *et al.*, "A generalised PID-type control scheme with simple tuning for the global regulation of robot manipulators with constrained inputs," *Int. J. Control*, vol. 88, no. 10, pp. 1995–2012, Feb. 2015.

[9] M. Alam and S. Celikovsky, "On the internal stability of non-linear dynamic inversion: Application to flight control," *IET Control Theory Appl.*, vol. 11, no. 12, pp. 1849–1861, Aug. 2017.

[10] S. Zhang, M. Lei, Y. Dong, and W. He, "Adaptive neural network control of coordinated robotic manipulators with output constraint," *IET Control Theory Appl.*, vol. 10, no. 17, pp. 2271–2278, Feb. 2016.

[11] Y. Yu, Z. Yang, C. Han, and H. Liu, "Fuzzy adaptive back-stepping sliding mode controller for high-precision deflection control of the magnetically suspended momentum wheel," *IEEE Trans. Ind. Electron.*, vol. 65, no. 4, pp. 3530–3538, Apr. 2018.

[12] M. R. Soltanpour, P. Otadolajam, and M. H. Khooban, "Robust control strategy for electrically driven robot manipulators: Adaptive fuzzy sliding mode," *IET Sci. Meas. Technol. Lett.*, vol. 9, no. 3, pp. 322–334, Feb. 2014.

[13] S. Liu, X. Guo, and L. Zhang, "Robust adaptive backstepping sliding mode control for six-phase permanent magnet synchronous motor using recurrent wavelet fuzzy neural network," *IEEE Access*, vol. 5, pp. 14502–14545, Feb. 2017.

[14] F. Zhang, "High-speed nonsingular terminal switched sliding mode control of robot manipulators," *IEEE/CAA J. Automatica Sinica*, vol. 4, no. 4, pp. 775–781, Feb. 2017.

[15] S. He and J. Song, "Finite-time sliding mode control design for a class of uncertain conic nonlinear systems," *IEEE/CAA J. Automatica Sinica*, vol. 4, no. 4, pp. 809–816, Feb. 2017.

[16] J. Baek, M. Jin, and S. Han, "A new adaptive sliding-mode control scheme for application to robot manipulators," *IEEE Trans. Ind. Electron.*, vol. 63, no. 6, pp. 3628–3637, Jun. 2016.

[17] Z. Zheng, Z. Jin, L. Sun, and M. Zhu, "Adaptive sliding mode relative motion control for autonomous carrier landing of fixed-wing unmanned aerial vehicles," *IEEE Access*, vol. 5, pp. 5556–5565, Feb. 2016.

[18] L. Wu, Y. Gao, J. Liu, and H. Li, "Event-triggered sliding mode control of stochastic systems via output feedback," *Automatica*, vol. 82, pp. 79–92, Aug. 2017.

[19] Y. Zhao, Y. Shen, A. Bernard, C. Cachard, and H. Liebgott, "Evaluation and comparison of current biopsy needle localization and tracking methods using 3D ultrasound," *Ultrasonics*, vol. 73, pp. 206–220, Jan. 2017.

[20] J. Liu, Y. Gao, X. Su, M. Wack, and L. Wu, "Disturbance-observer-based control for air management of PEM fuel cell systems via sliding mode technique," *IEEE Trans. Control Syst. Technol.*, to be published. [Online]. Available: http://ieeexplore.ieee.org/document/8299459/, doi: 10.1109/TCST.2018.2802467.

[21] J. Liu, S. Vazquez, L. Wu, A. Marque, H. Gao, and L. G. Franquelo, "Extended state observer based sliding mode control for three-phase power converters," *IEEE Trans. Ind. Electron.*, vol. 64, no. 1, pp. 22–31, Jan. 2017.

[22] F. Abdelhedi and N. Derbel, "Adaptive second order sliding mode control under parametric uncertainties: Application to a robotic system," *Int. J. Model. Identificat. Control*, vol. 27, no. 4, p. 322, Feb. 2017.

[23] A. Bessas, A. Benalia, and F. Boudjema, "Integral sliding mode control for trajectory tracking of wheeled mobile robot in presence of uncertainties," *J. Control Sci. Eng.*, vol. 2016, Feb. 2016, Art. no. 7915375.

[24] J. Liao, Z. Chen, and B. Yao, "Performance-oriented coordinated adaptive robust control for four-wheel independently driven skid steer mobile robot," *IEEE Access*, vol. 5, pp. 19048–19057, Feb. 2017.

[25] B. Li, X. Zhang, Y. Fang, and W. Shi, "Visual servo regulation of wheeled mobile robots with simultaneous depth identification," *IEEE Trans. Ind. Electron.*, vol. 65, no. 1, pp. 460–469, Jan. 2018.

[26] R. S. Ortigoza, J. R. G. Sanchez, V. M. H. Guzman, C. M. Sanchez, and M. M. Aranda, "Trajectory tracking control for a differential drive wheeled mobile robot considering the dynamics related to the actuators and power stage," *IEEE Latin Amer. Trans.*, vol. 14, no. 2, pp. 657–664, Feb. 2016.

[27] J. Jiang, P. Di Franco, and A. Astolfi, "Shared control for the kinematic and dynamic models of a mobile robot," *IEEE Trans. Contr. Syst. Technol.*, vol. 24, no. 6, pp. 2112–2124, Nov. 2016.

[28] M. T. Nasir and S. El-Ferik, "Adaptive sliding-mode cluster space control of a non-holonomic multi-robot system with applications," *IET Control Theory Appl.*, vol. 11, no. 8, pp. 1264–1273, May 2017.

CHUNBO XIU received the Ph.D. degree in navigation, guidance and control from the Beijing Institute of Technology, Beijing, China, in 2005. His research interests include neural networks, system modeling, and chaos control.

RUOSI WANG received the B.S. degree in control science and engineering from the Hebei University of Architecture, Zhangjiakou, China, in 2016. Her research interests include sliding mode control and neural network.